Flashback and Turbulent Flame Speed Measurements in Hydrogen/Methane Flames Stabilized by a Low-Swirl Injector at Elevated Pressures and Temperatures

David Beerer
e-mail: djb@ucicl.uci.edu

Vincent McDonell[1]
e-mail: vgm@ucicl.uci.edu

UC Irvine Combustion Laboratory
Irvine, CA 92697-3550

Peter Therkelsen
e-mail: ptherkelsen@lbl.gov

Robert K. Cheng
e-mail: rkcheng@lbl.gov

Lawrence Berkeley National Laboratory
Berkeley, CA 94720

This paper reports flashback limits and turbulent flame local displacement speed measurements in flames stabilized by a low swirl injector operated at elevated pressures and inlet temperatures with hydrogen and methane blended fuels. The goal of this study is to understand the physics that relate turbulent flame speed to flashback events at conditions relevant to gas turbine engines. Testing was conducted in an optically accessible single nozzle combustor rig at pressures ranging from 1 to 8 atm, inlet temperatures from 290 to 600 K, and inlet bulk velocities between 20 and 60 m/s for natural gas and a 90%/10% (by volume) hydrogen/methane blend. The propensity of flashback is dependent upon the proximity of the lifted flame to the nozzle that is itself dependent upon pressure, inlet temperature, and bulk velocity. Flashback occurs when the leading edge of the flame in the core of the flow ingresses within the nozzle, even in cases when the flame is attached to the burner rim. In general the adiabatic flame temperature at flashback is proportional to the bulk velocity and inlet temperature and inversely proportional to the pressure. The unburned reactant velocity field approaching the flame was measured using a laser Doppler velocimeter with water seeding. Turbulent displacement flame speeds were found to be linearly proportional to the root mean square of the velocity fluctuations about the mean velocity. For identical inlet conditions, high-hydrogen flames had a turbulent flame local displacement speed roughly twice that of natural gas flames. Pressure, inlet temperature, and flame temperature had surprisingly little effect on the local displacement turbulent flame speed. However, the flow field is affected by changes in inlet conditions and is the link between turbulent flame speed, flame position, and flashback propensity. [DOI: 10.1115/1.4025636]

Introduction

Operation of gas turbines on synthesis gas from gasification of coal is of interest as a means to reduce the carbon intensity of this fuel [1]. Additionally, use of gasified biomass can also be considered. Depending upon the source of coal and the synthesis process, hydrogen concentrations in the resulting gas stream can be upwards of 90% by volume [1]. Several studies in past years have outlined the difficulty of stabilizing high-hydrogen flames in lean premixed combustors. The prominent challenge is associated with hydrogen's high reactivity, which makes the flame prone to flashback into the premixer [2].

Avoiding operating conditions that lead to flashback is of paramount importance to combustion engineers. Unfortunately, design guides and other tools developed to help predict the propensity of flashback are in their infancy. The interaction of the turbulent flame propagation rate with the flow field aerodynamics is a complex process, making it difficult to model. Numerical simulations of hydrogen/air flames detailing the interaction of wrinkled flames with the flow have been reported [3,4]. These high fidelity simulations are very time consuming and computationally expensive, limiting their application in engineering design. Turbulent flame speed measurements can be found in the literature [5,6], though only a handful were obtained at elevated pressures and temperatures relevant to gas turbine combustors [7,8]. However, a knowledge gap still exists on how to use such information for the accurate prediction of flashback in a lean premixed combustor.

In a low-swirl combustor a divergent turbulent flow field stabilizes a freely propagating detached lifted flame. The divergent flow field is produced with a device known as a low-swirl injector (LSI) that is placed inside the premixer typically 1 to 1.5 diameters upstream of the nozzle exit. The LSI consists of an inner channel with a perforated plate and an outer annulus containing multiple swirl vanes, as shown in Fig. 1. Premixed reactants pass through the annulus and the center section. Reactants passing through the annulus form a swirling outer region in the combustor, while the reactants passing through the inner channel form a non-swirling inner region. The hole pattern and sizes on the perforated plate control the level of turbulence developed in the inner flow as well as the flow split between inner and outer regions. The swirling motion of the outer flow causes it to expand radially outward, which induces a similar divergence on the inner flow as well. The divergence results in a decreasing mean axial velocity along the centerline of the flow field. This velocity gradient is the key to stabilizing the flame. When lit, the turbulent flame propagates

[1]Corresponding author.

Contributed by the Combustion and Fuels Committee of ASME for publication in the Journal of Engineering for Gas Turbines and Power. Manuscript received July 2, 2013; final manuscript received September 16, 2013; published online November 5, 2013. Assoc. Editor: Klaus Dobbeling.

Fig. 1 Low-swirl injector, back view (left) and front view (right)

against the velocity gradient at a characteristic speed $S_{T,LD}$ until it reaches a point along the axis where the local velocity U is equal in magnitude but opposite in direction to $S_{T,LD}$ [9]. The two velocities will balance, resulting in a stationary lifted flame. Figure 2 shows a lifted methane/air flame from the current study with illustrative streamlines of the flow field superimposed. Flow is from top to bottom. The distance between the exit plane of the nozzle (defined as $x = 0$) and the leading edge of the flame (denoted as x_f) is known as the lift-off height. As will be shown later, $S_{T,LD}$ is primarily only a function of the fuel composition and u', the root mean square of the turbulent velocity about the mean. The mean strain from the flow divergence keeps u' fairly constant along the axis from the nozzle exit to the flame front.

Unlike high swirl burners, the LSI does not impart enough swirl to form a vortex breakdown or central recirculation zone within the vicinity of the flame. As a result, the simpler aerodynamics of this flow lends itself to very straightforward analytical models of the premixed turbulent flame process and flame position [9]. Additionally, the lifted flame does not interact with the combustor wall minimizing heat transfer to the nozzle [10]. As will be shown later, this results in the flashback mechanism to be dominated by the aerodynamics in the core flow rather than by heat transfer or boundary layer effects. Being lifted, the entire flame is optically visible, making it more accessible for interrogation with optical or laser diagnostics [9].

The LSI concept was initially developed as a convenient means of studying fundamental turbulent flame properties in a laboratory setting, [11]. Experience has found that this flame can stabilize a number of fuels over a wide range of conditions, while maintaining low emissions [12]. Low-swirl burners have, subsequently, been developed for atmospheric pressure applications such as industrial furnaces, boilers, and heaters of various sizes and power outputs [13].

Recently, interest has begun in developing this technology for fuel flexible gas turbines [14]; however, this requires knowledge of the flame's performance and properties at elevated pressures and temperatures. So far, only a handful of studies have been conducted with the LSI at representative gas turbine conditions. Solar Turbines® and Lawrence Berkeley National Laboratories (LBNL) performed single nozzle rig tests with natural gas at pressures P_o, inlet temperatures T_o, and bulk velocities U_o of up to 13 atm, 700 K, and 48 m/s, respectively. Emissions and blow out limits were reported in Johnson et al. [15] and Nazeer et al. [16]. The National Energy Technology Lab (NETL) also studied the LSI in its optically accessible SimVal combustor test rig at similar conditions with fuel mixtures of methane and hydrogen. Flame imaging, emissions, and limited flashback measurements were reported in Cheng et al. [17]. Finally, Georgia Tech conducted experiments with several syngas compositions at elevated pressure conditions. Noble et al. [18] reports flame images, emissions, and lean blowout (LBO) measurements from this work illustrating the operability of LSI concept on syngas at gas turbine conditions.

The most challenging class of fuel reported in these studies is that containing high concentrations of hydrogen. Cheng and Littlejohn [19] have reported that, at equivalence ratios φ above 0.3

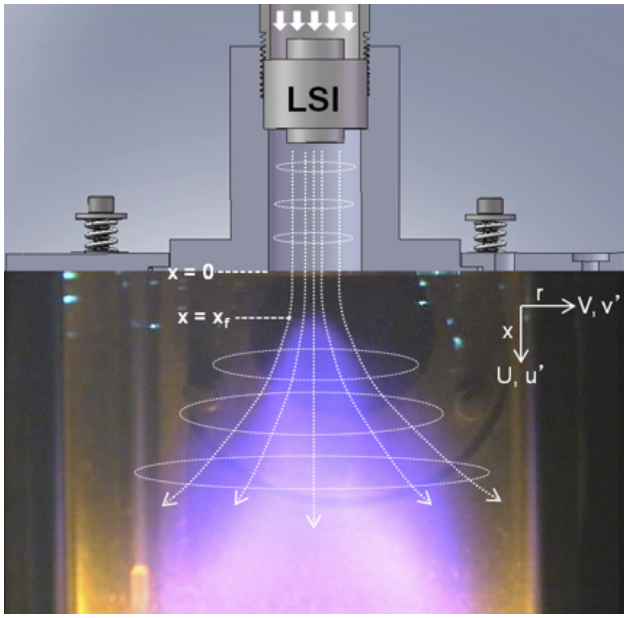

Fig. 2 Low-swirl methane flame with illustrative streamlines superimposed. The diverging lines represent the inner flow, while the ellipses represent the swirling outer flow. Flow direction is top to bottom.

for hydrogen, flames have a tendency to begin burning in the shear layer. When this occurs, the flames fold back and attach to the burner rim; however, the inner region of the flame still remains lifted. Later research found that flashback could occur at high enough firing temperatures for hydrogen fuel concentrations in excess of 80% [17]. Their limited data indicate that increasing hydrogen concentration increases the propensity for flashback; however, the influence of P_o, T_o, and U_o was not explored. It is also uncertain if the flame flashed back through the inner region or the outer shear and boundary layer. The former is more common for high-swirl flames, while the latter is more common for jet flames [20,21]. Experimental studies of hydrogen combustion in gas turbine engines confirm these challenges [22].

The goal of this study is to extend the previous work by elucidating the physics relating turbulent flame speeds to flashback at conditions relevant to gas turbine engines. In the present investigation, velocities and flashback limits are measured in a flame stabilized by a low-swirl injector (LSI) at elevated pressures and inlet temperatures. Through the use of laser Doppler velocity (LDV) local displacement turbulent flame speed data have been obtained at gas turbine relevant conditions that can be compared directly with those obtained at atmospheric conditions. With this information the relationships between the inlet conditions, flow field, turbulent flame speed, and flashback propensity are established at conditions relevant to gas turbine engines.

Experiment

Experiments were performed in an optically accessible high-pressure vessel at the University of California Irvine Combustion Laboratory (UCICL). A photograph of the facility is shown in Fig. 3 and full details are given elsewhere [23,24]. High temperature pressurized air is supplied by air compressors and electric resistance heaters. A back-pressure valve regulates the test section pressure. The test vessel pressure, inlet temperature, air, and fuel flows are all independently adjusted and controlled through proportional integral derivative (PID) feedback control loops.

A cross-sectional image of the high-pressure vessel is shown in Fig. 4. The vessel itself is made from a 40.6 cm (16 in.) schedule-40 chrome-moly steel pipe with 40.6 cm (16 in.)-136 kg (300 lb.) flange ends. The vessel contains two pairs of window ports.

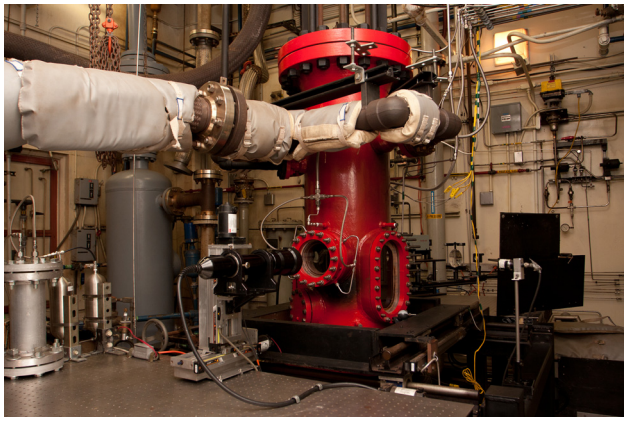

Fig. 3 High-pressure vessel and facility

One pair is for 15.3 cm (6 in.) in diameter circular windows, while the other is for 20 cm by 15.5 cm (8 in. × 6 in.) oblong windows. Windows are made from 5 cm (2 in.) thick fused silica.

The pressure vessel houses a single LSI nozzle combustor configuration. The combustor liner/test section consists of a quartz tube 15 cm (6 in.) in diameter, 3 mm thick, and 23 cm (9 in.) in length. The tube is compressed between two stainless steel plates that are rigidly held into place with four posts. Graphite gaskets are used to produce a leak-free fit between the quartz tube and the metal, even at the high flame temperatures. Springs are located at the end of each post to allow the combustor liner to grow from thermal expansion.

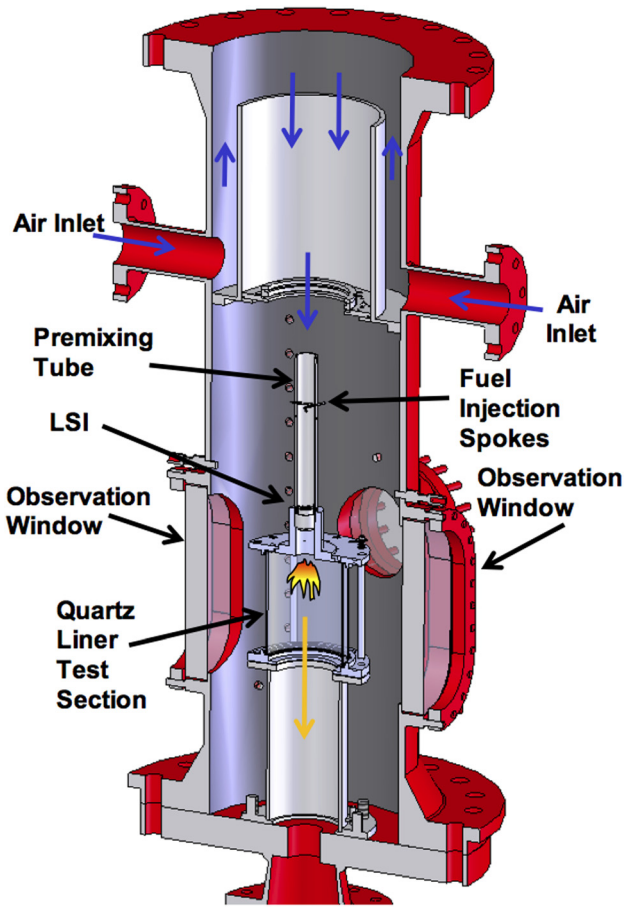

Fig. 4 Cross-sectional image of pressure vessel and combustor test section

The premixing chamber consists of a 3.17 cm (1.25 in.) stainless steel pipe, 30 cm (12 in.) in length with three fuel spokes positioned perpendicular to the flow near the inlet (top) of the tube. Two sets of thermocouples are used for flashback detection. One set is mounted flush within the walls of the nozzle, while the other set is located in the premixer just downstream of the fuel injection spokes. Additionally, pressure ports in the premixer and combustor allow for measurements of the pressure drop across the LSI and flame during testing. The pressure drop is also used to detect flashback.

The LSI used in the present study is shown in Fig. 1. The outer and inner channel radii (R_o, R_i) are 19 mm and 13 mm, respectively. The LSI has 16 aerofoil-shaped swirl vanes with a discharge angle of 37 degrelative to the incoming flow. This LSI design is a scaled down version of the one used by NETL [17] and more recently by Therkelsen et al. [25]. The same LSI is used throughout this study but with two different perforated plates. The first plate (LSI-P1) has a thickness of 1.5 mm, while the second plate (LSI-P2) has a thickness of 1.3 mm. The perforated plate consists of 25 holes about 2.6 mm in diameter arranged in a concentric pattern. The two plates achieve different flow splits through the LSI, which will be discussed in more detail later.

A closed-loop water circuit quenches the hot exhaust products after they exit the combustor test section. Two computers located in the adjacent control room collect and record all pertinent data using National Instruments LABVIEW® software.

Fuel flow is controlled either manually with a needle valve or via a dual-fuel mixing station. Two Alicat® mass flow controllers, installed in parallel, meter the fuel flow rate. By adjusting the flow rate of each gas, binary mixtures of the constituent fuels can be established and tested in the rig. Natural gas (with nominal composition ~97% CH_4, 1% C_2H_6, 2% CO_2, and N_2) is supplied from a gas compressor while other gases are supplied from high-pressure cylinders. Maximum flow rates of natural gas and H_2 are 15 g/s and 3.5 g/s, respectively. The air flow rate is measured with a FCI® ST98-L thermal mass flow meter, which has roughly a 2% measurement uncertainty. The fuel flow is also measured through two Micromotion® CMF010 Coriolis meters, each with a 0.5% uncertainty. The stated equivalence ratio and firing temperature are, therefore, known to within about 3% and the stated inlet pressure and temperature are known to within about 0.1 atm and 5 K, respectively. Ignition is accomplished nonintrusively from focusing the beam from a frequency doubled Nd:YAG laser fired at 10 Hz into the central vicinity of the test section. The laser can be seen in the background of Fig. 3 and is fired into the vessel through one of the circular quartz windows not used for diagnostic purposes.

Flow field measurements are made with a two-color laser Doppler velocimeter (LDV) system using water droplets for seeding. Seed particles are formed by injecting water through a small BETE® Model PJ8 fogging nozzle mounted above the premixer. The droplets average (D_{10}) 10 microns in diameter and are entrained within the air. The heated air results in substantial evaporation of the droplets; thus, the particle sizes at the measurement location are generally less than 5 μm in diameter. Based on air and water flow rates, the water mass fraction to air is usually less than 1%. A Coherent I-90 C 4-watt argon ion laser is used to generate a laser beam that is sent to a TSI® FBL-2 multicolor beam generator, which separates the beam into green (514.5 nm) and violet (476.5 nm) beams. The beams pass through a fiber optic cable to a TSI® TR-260 transceiver mounted on a two-direction traverse adjacent to one of the oblong quartz windows. The transceiver is shown in the foreground in Fig. 3. The beams are focused in the test section using a 500 mm focal length lens in the transceiver. The green beams are used to measure the vertical (axial) velocity, and the violet beams measure the horizontal (transverse) velocity. The back-scattered light is collected by the transceiver and sent via a fiber optic cable to a TSI® PDM-1000 photomultiplier module. The analog signal is filtered, digitized, and

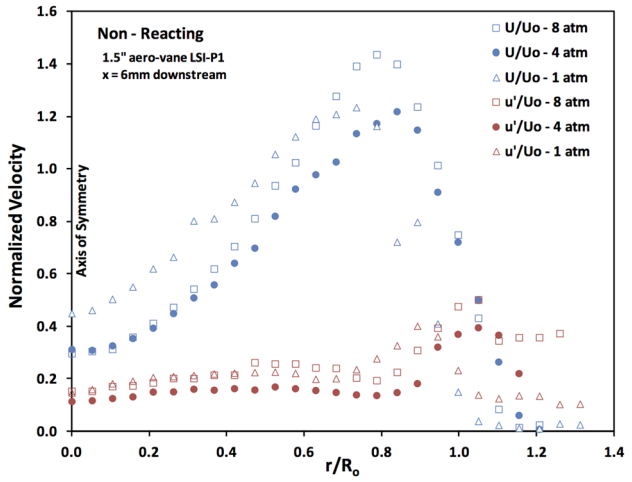

Fig. 5 Nonreacting radial profiles of normalized mean and rms axial velocities for LSI-P1. (Inlet conditions: $P_o = 1–8$ atm, $T_o = 380–470$ K, $U_o = 25–47$ m/s.)

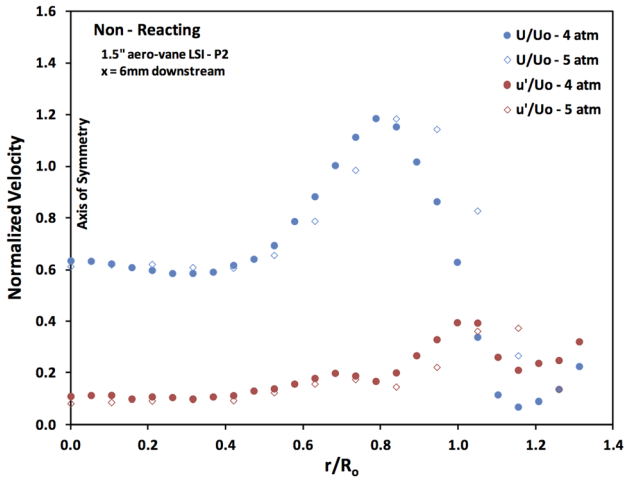

Fig. 6 Nonreacting radial profiles of normalized mean and rms axial velocities for LSI-P2. (Inlet conditions: $P_o = 4–5$ atm, $T_o = 440–450$ K, $U_o = 35–48$ m/s.)

processed with a TSI® FSA-4000 signal processor and the results are recorded on a computer.

Results

Nonreacting Flow Field. Experimental results are reported in terms of the inlet pressure P_o, inlet mixture temperature T_o, bulk velocity U_o, and adiabatic flame temperature (*AFT*). U_o is calculated by dividing the volumetric flow rate of air and fuel through the premixer by its cross-sectional area, 11.4 cm^2. T_o is calculated from an energy balance based on the inlet temperatures and flow rates of the air and fuel. *AFT* is calculated based on P_o, T_o, fuel composition, and equivalence ratio φ, using the equilibrium module in Reaction Design's CHEMKIN® software.

Nonreacting radial profiles of the axial velocities for LSI-P1 and LSI-P2 are shown in Figs. 5 and 6, respectively. These measurements are made 6 mm downstream of the nozzle exit (i.e., at $x = 6$ mm). Laser access for $x < 6$ mm is prevented by interference of the upper beam with the exit plane. The profiles are normalized by U_o and R_o. Qualitatively, the flow profiles are similar to those measured by Cheng et al. [9] at atmospheric pressures. The mean velocity, U/U_o, in the inner region ($r/R_o < 0.6$) is less than the velocity through the outer region ($r/R_o > 0.6$). The turbulence intensity u'/U_o is relatively uniform in the inner region, around 10%, but increases to 40% around $r/R_o = 1$, indicating the presence of a shear layer at the burner rim [26].

The filled symbols in Figs. 5 and 6 have similar inlet conditions to allow comparison of the flow field generated by LS1-P1 and LSI-P2. The LSI-P1 mean velocity profile is parabolic in shape, with $U/U_o = 0.3$ at the centerline. The LSI-P2 profile has a much flatter inner region, with higher velocities at the centerline, $U/U_o = 0.6$. Conversely, the peak velocity in the outer region for LSI-P1 is higher, $U/U_o = 1.4$, compared to LSI-P2 with a peak $U/U_o = 1.2$. These results indicate that LSI-P2, with the thinner perforated plate, has a higher fraction of air passing through the inner channel.

Comparison of the flow fields at different operating pressures (filled-in versus open symbols in each respective plot) indicates that U/U_o at the centerline decreases with increasing pressure. Subsequently, the mean velocities in the outer region increase with pressure. This indicates that the flow split is somewhat dependent upon the pressure. Curiously, u'/U_o does not show a pressure dependency. Unfortunately, due to temperature limitations with the water seed droplets (the drops completely evaporate at the higher temperatures), the effect of T_o on flow split could not determined. Measurements at higher bulk velocities indicated that U/U_o and u'/U_o are invariant with flow rate. This is consistent with the self-similar flow properties that Cheng et al. [9] reported at atmospheric conditions.

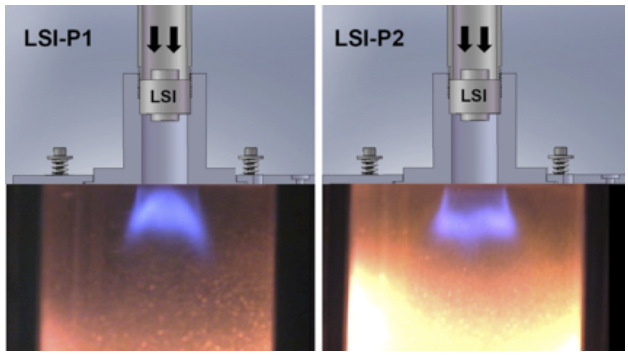

Fig. 7 Images of 90%/10% hydrogen/methane flames from LSI-P1 and LSI-P2 at similar inlet conditions ($P_o = 3$ atm, $T_o = 294$ K, $U_o = 45$ m/s, *AFT* = 1870 K)

Flame Shape. Figure 7 compares images of the flames generated using both LSI configurations with the 90%/10% H_2/CH_4 fuel blend. LSI-P1 has a parabolic-shaped flame in the inner region while the LSI-P2 flame is flatter. The LSI-P1 flame anchors closer to the nozzle rim (i.e., a smaller x_f) due to the lower velocity at the centerline compared to LSI-P2. The flat inner region of the LSI-P2 flame has been observed in high-hydrogen flames at atmospheric pressure [27]. The higher mean velocity in the outer region of LSI-P1 pushes the edge of the flame back, resulting in only a small amount of burning in the shear layer. Conversely, the lower mean velocity in the outer region of LSI-P2 leads to a more prominent flame in the shear layer. As will be seen in the next section, the flame shape and position have a major influence on the flashback propensity for both configurations.

Testing was conducted at different inlet and firing conditions (P_o, T_o, U_o, and *AFT*) to see how each parameter affected the flame front position x_f. When increasing either P_o or *AFT*, while keeping the other variables fixed, decreased x_f. Conversely, increasing either T_o or U_o correspondingly increased x_f. Photographs of flames at different inlet conditions that show these trends can be found in Beerer [24].

Flashback. Flashback limits for both LSI configurations were measured using the high-hydrogen fuel blend of 90%/10% $H_2/$

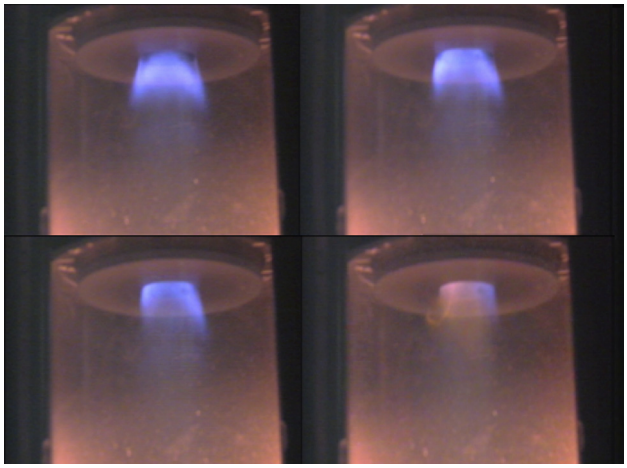

Fig. 8 Sequential images of a flashback event

CH_4, by volume. The flashback limit was determined for each test by first establishing a relatively low flame temperature ($AFT \approx 1200$ K) in the combustor. Then, while keeping P_o, T_o, and U_o constant, the equivalence ratio (and AFT) was gradually increased until the flame flashed back. At this point the fuel flow was terminated. Test conditions ranged from: $3\text{ atm} < P_o < 8\text{ atm}$, $290 < T_o < 600$ K, $20\text{ m/s} < U_o < 60\text{ m/s}$. Under these same conditions, natural gas flames were never observed to flashback.

As AFT increased, the flame drew closer to the nozzle (i.e., $x_f \rightarrow 0$). Flashback occurred once the leading edge of the flame reached the nozzle ($x_f = 0$) for both configurations. Figure 8 shows a sequence of photographs from a flashback using LSI-P1. From studying these images and those from other tests, it appears that flashback occurs via flame propagation through the central region of the flow, even at conditions where a flame appears in the shear layer. In the second photograph (upper right image), for instance, the flame core is well within the nozzle, but a gap still exists between the flame and the rim. This suggests the flame did not propagate through the shear layer/boundary layer. Only in the final photograph (lower right image) when the flame is fully flashed back does the flame also encompass the boundary layer region.

Flashback could be observed visually, prompting the operator to manually terminate fuel flow. Thermocouples mounted in the nozzle and premixer wall measured a temperature rise after flashback, but their response time was fairly slow (on the order of seconds). The pressure drop measured between the premixer and combustor also registered a sudden increase (within tenths of second) after flashback, as shown in Fig. 9. Because of the faster response time, the LabView® controller was programmed to automatically terminate the fuel flow when the pressure drop value increased by a factor of two over the steady value for the flow in a nonreacting condition, i.e.,

$$\Delta p_{\text{flashback}} > 2 \cdot \Delta p_{\text{non-reacting}}$$

Generally the pressure drop for a stable flame is about 20% higher than that for the corresponding nonreacting flow. This method proved to be a reliable means of sensing flashback and automatically terminating fuel flow before the flame damaged the LSI.

Figure 9 also shows the corresponding axial velocity in the combustor during a flashback event. The velocity measurements were made using the LDV system at $x = 15$ mm along the combustor centerline downstream of the sudden expansion. The mean velocity is steady until flashback, at which point it rapidly increases. Upon termination of the fuel, the velocity drops back to its nominal preflashback range. The velocity remains positive during the entire event, at no time does a velocity dip or flow reversal occur. This indicates that no recirculation bubble or vortex break down precedes flashback, suggesting that the combustion-induced vortex break (CIVB) flashback mechanism, common for high-swirl burners [20], does not contribute to flashback in a low-swirl burner. The lack of any pressure or velocity oscillations also negates the possibility of a combustion instability induced flashback. Inspections of the LSI after flashback showed discoloration on the downstream face of the perforated plate, indicating that the flame attaches to the LSI perforated plate upon flashback. Once this occurs, the flow through the nozzle is mostly hot combustion products, rather than unburned reactants. The hot combustion products have a lower density and, subsequently, a higher velocity, which would explain the observed velocity increase and pressure drop surge in Fig. 9 during flashback.

Figure 10 shows the flashback results from this study for LSI-P1 using the 90%/10% H_2/CH_4 blend at $T_o = 400$ K. The symbols represent the AFT where the flashback occurred for a given P_o and U_o. Tests at common pressures are connected with straight lines. Regions where a flame can be successfully stabilized exist below each line; the flame is prone to flashback above the lines. The results indicate that, for a constant T_o and P_o, increased U_o increases the AFT at flashback occurs. At higher pressures this U_o dependency (slope) decreases. For a constant T_o and U_o, increasing P_o decreases the AFT at which flashback occurs. This flashback dependency on U_o and P_o is similar to that observed in high-swirl and jet burners [28–31].

Figure 11 compares the flashback limit of LSI-P1 for varying inlet temperatures. For a constant U_o and P_o, increasing T_o increases the AFT at which flashback occurs. This is rather surprising because studies with high-swirl and jet burners report that increasing T_o decreases the flashback limit [28,31]. This is an important finding because it indicates that, in a simple-cycle gas turbine, where T_o increases with pressure ratio, the detrimental effect that the increase in P_o has on the flashback limits will be, in part, counterbalanced by the observed beneficial effect of

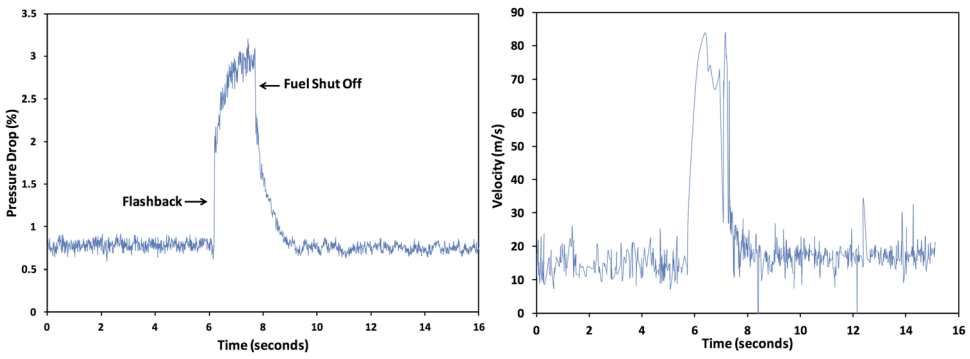

Fig. 9 Pressure drop and axial velocity measurements during a flashback event

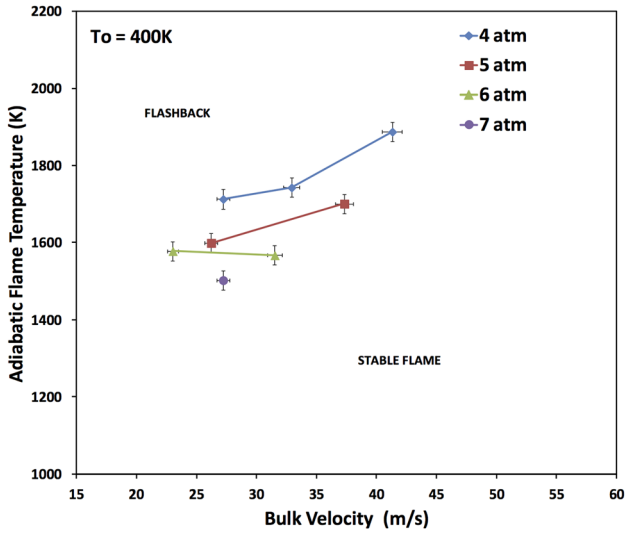

Fig. 10 Flashback results for LSI-P1 for $T_o = 400$ K

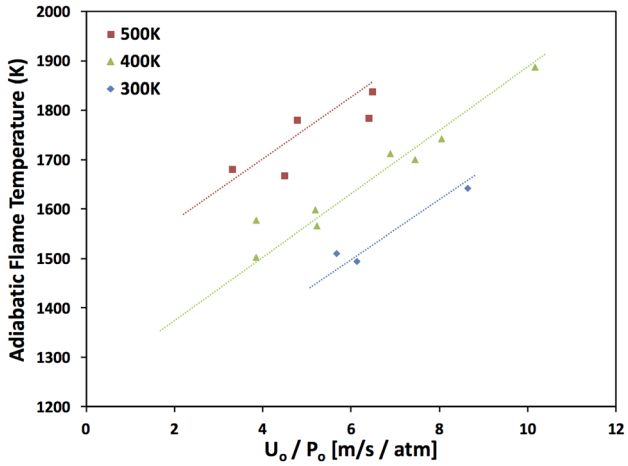

Fig. 11 Effect of T_o on flashback limit for LSI-P1

increasing T_o. As a result, the flashback propensity for the LSI-stabilized reaction should be reduced compared to either high-swirl or jet burners for engines with high overall pressure ratios.

Based on the dependency of the flashback limit on the inlet conditions, the data for LSI-P1 were regressed into an expression for equivalence ratio, or φ, at flashback as a function of U_oT_o/P_o

$$\varphi_{\text{flashback}} = A \cdot \left(\frac{U_o^{[\frac{m}{s}]} T_o^{[K]}}{P_o^{[\text{atm}]}} \right) + B \quad (90/10\text{H}_2/\text{CH}_4) \qquad (1)$$

for LSI-P1, $A = 6.51 \times 10^{-5}$ and $B = 0.336$. Figure 12 shows that the flashback results collapse quite well with the correlation; the average error between the actual and predicted values is $\pm 3\%$. The data correlated better with φ than AFT, which is why φ was used in the correlation. Thus, by specifying the U_o, T_o, and P_o for a given engine, the value of φ at flashback can be easily calculated. The AFT for the 90%/10% H_2/CH_4 blend under lean conditions can then be calculated using the empirical formula

$$AFT = C \cdot T_o^{[K]} + D$$

where

$$C = -0.343\varphi + 0.978$$

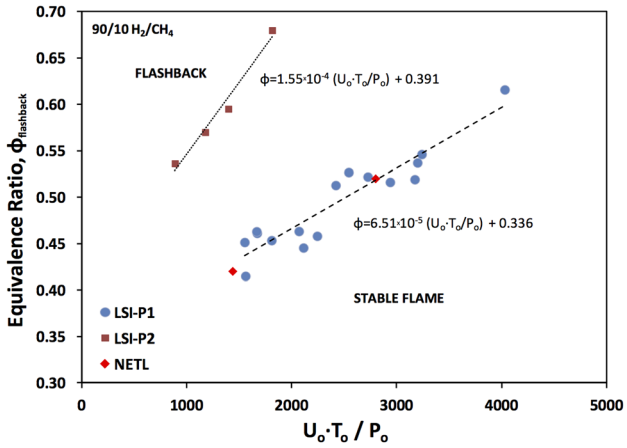

Fig. 12 Correlation for flashback limit of LSI-P1

and

$$D = -1007\varphi^2 + 3132\varphi + 38.9$$

This formula is accurate to within ± 5 K compared to temperatures calculated in CHEMKIN® for $1200\,\text{K} < AFT < 1900\,\text{K}$ at any pressure.

To help assess the generality of the expression derived for the present work, two of the conditions where NETL encountered flashback are also shown in Fig. 12. In NETL's tests, the hydrogen concentration in the fuel was increased while holding P_o, T_o, U_o, and φ constant until flashback occurred [17]. The two points represent conditions where flashback occurred with hydrogen concentrations of roughly 90%. NETL's two points fall onto the correlation line from this study, which uses a similar LSI design. This indicates that flashback conditions are repeatable in different combustors/facilities. NETL also reported that, for a fixed inlet conditions, increasing the hydrogen concentration decreased the flashback limit. Therefore, it should be emphasized that the correlation in Fig. 12 is strictly for the 90%/10% H_2/CH_4 blend. Comparison of the NETL data with the correlation from the present study indicates that, for 100% H_2, flashback occurs at an AFT approximately 350 K lower than that for the corresponding 90%/10% H_2/CH_4 blend. Most likely, the dependency of flashback on P_o, T_o, and U_o observed in this study also holds for varying levels of hydrogen concentration.

The video evidence presented earlier in this section shows that flashback occurs when the leading edge of the flame ingresses into the nozzle, or $x_f \to 0$. This would suggest that, if the lift-off height could be increased, the flashback resistance of the burner would be improved. This was tested by measuring the flashback limits of LSI-P2, which from Fig. 7, is seen to have a larger lift-off height due to the higher fraction of flow through the inner channel. A handful of tests were conducted with LSI-P2 and are plotted in Fig. 12. On average, LSI-P2 could stabilize flames at an AFT about 300 K higher than LSI-P1. A correlation of the same form was developed for LSI-P2, with $A = 1.55 \times 10^{-4}$ and $B = 0.391$. In spite the greater burning intensity in the shear layer, the results support the hypothesis that flashback is controlled by the flame position in the inner region alone and is not influenced by the flame attachment at the burner rim.

The flashback results with LSI-P2 might, at first, suggest it is a preferable design over LSI-P1. However, while the LSI-P2 does provide better flashback resistance, it had difficulty stabilizing natural gas flames. As seen in Fig. 2, the lift-off height for the methane flames with LSI-P1 is nominally around $x_f \approx 5$ mm at typical operating conditions from this study. For LSI-P2, $x_f \approx 50$ mmfor the natural gas flames at similar inlet conditions due to the higher velocities in the inner region. At a distance that far

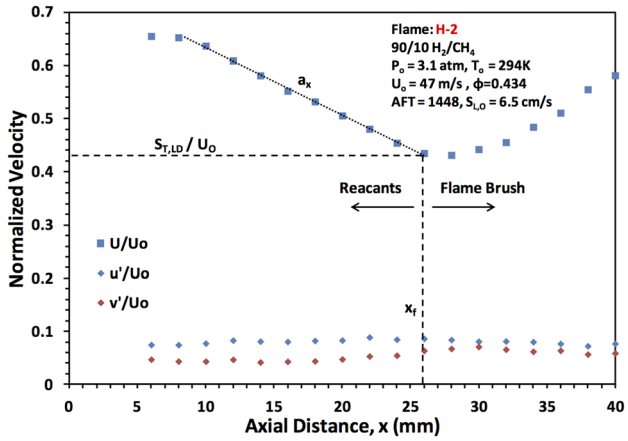

Fig. 13 Axial profiles of normalized mean, rms axial and rms radial velocities for a high-hydrogen flame with LSI-P2

downstream of the nozzle the shear layer mixes with the inner region, which raises the turbulence intensity and disrupts the flow divergence. As a result, natural gas flames with LSI-P2 were observed to fluctuate wildly around the mean lift-off height, leading to severe pressure oscillations. In short, while the LSI-P2 design is optimized for high-hydrogen operation, LSI-P1 is more fuel-flexible. The ideal configuration for an engine would likely fall in between these two designs.

Turbulent Flame Speed. In low-swirl flames, the local displacement turbulent flame speed $S_{T,LD}$ is the most relevant turbulent flame speed for investigation [1,9]. This is the speed at which the leading edge of the flame propagates into the flow. By measuring the velocity at the leading edge of the flame, the turbulent flame speed can be deduced, $U|_{x=x_f} = S_{T,LD}$ per the definition given by Cheng et al. [9].

The velocities in the reacting flows were measured just along the centerline ($r = 0$) of the combustor. LSI-P1 was used for the natural gas flames because of its good stability; while LSI-P2 was used for the high-hydrogen flames to take advantage of the larger lift-off height. Because water droplets are used for seeding, which evaporate upon entering the flame front, these are *conditioned* velocity measurements [32]. In other words, the measured velocities can only be those associated with the unburned reactants, both upstream and through the flame brush. Figure 13 presents the axial profile of the normalized mean and the rms fluctuating velocity components for a reacting flow. U/U_o initially decreases linearly from the nozzle exit ($x = 0$) to the flame front x_f; it then increases through the flame brush. While not shown, the signal data rate upstream of x_f is relatively constant but decreases rapidly upon entering the flame brush. The axial and transverse rms velocities u' and v' increase by about 5% from $x = 0$ to x_f. The magnitude of v' is roughly half that of u'. Overall, these profiles are very similar to the reacting profiles observed by Cheng et al. [9] atmospheric pressure.

Turbulent displacement flame speeds $S_{T,LD}$ were deduced for natural gas, 90/10 H_2/CH_4 blend, and pure hydrogen flames from the axial profile measurements over a range of inlet conditions: $3\,\text{atm} < P_o < 8\,\text{atm}$, $290 < T_o < 420\,\text{K}$, $20\,\text{m/s} < U_o < 60\,\text{m/s}$. For the combustor used, these conditions correspond to flames with thermal power outputs from 190 to 390 kW. The *AFT* for the natural gas and high-hydrogen flames ranged from 1780 K to 1950 K and 1350 K to 1770 K, respectively. The full details of the conditions for each burn test are listed in Table 1. It is noted that the firing temperature range was primarily limited by the lean blow out and flashback points.

The $S_{T,LD}$ results are shown in Fig. 14 as a function of u' measured at x_f. The measurements from the current study are shown as circles, while the results from Cheng et al. [2,19] at standard atmospheric conditions are displayed as diamonds. The estimated error from this study are $\pm 2\%$ for the $S_{T,LD}$ and $\pm 10\%$ for u' based on a 95% confidence level. Typically 2000 to 3000 velocity samples were taken for each test point.

Cheng et al. [9] reports that $S_{T,LD}$ scales linearly with u'. The measurements from the present study indicate that this linear relation continues to hold at elevated pressures, temperatures, and turbulence intensities as well. The entire set of data correlates well with the relation

$$S_{T,LD} = K \cdot u'$$

where $K_{H_2/CH_4(90/10)} = 4.2$, and $K_{CH_4} = 2.1$. This simple relation is rather remarkable given the wide range of inlet conditions and firing temperatures in this study. The lack of any pressure, inlet temperature, equivalence ratio/firing temperature dependency

Table 1 Test Conditions for LDV testing of methane, high-hydrogen and nonreacting flows

Test	Aero vane LSI	Fuel	P_o (atm)	$\dot{m}_{air}$ (g/s)	Bulk velocity (m/s)	T_o (K)	Equivalence ratio	*AFT* (K)	CH_4 (%)	H_2 (%)	u' (m/s)	S_T (m/s)	x_f (mm)	a_x (1/mm)	x_o (mm)
Reacting															
C-1	Original	CH_4	3.1	164.2	40.0	294	0.764	1933	100.0	0.0	3.23	7.96	9	−0.0102	−70
C-2	Original	CH_4	4.0	161.7	31.1	294	0.754	1920	100.0	0.0	2.98	6.26	6	—	—
C-3	Original	CH_4	5.0	173.9	26.8	294	0.669	1779	100.0	0.0	2.90	6.08	6	—	—
C-4	Original	CH_4	3.1	149.2	37.8	294	0.755	1923	100.0	0.0	3.36	8.01	6	—	—
C-5	Original	CH_4	3.1	170.6	58.4	392	0.710	1918	100.0	0.0	6.06	14.18	7	−0.0156	−42
C-6	Original	CH_4	3.5	185.5	59.1	417	0.719	1950	100.0	0.0	6.14	13.24	6	−0.0147	−47
C-7	Original	CH_4	4.1	185.6	50.5	418	0.715	1943	100.0	0.0	5.79	11.77	7	—	—
Reacting															
H-1	Modified	H_2/CH_4	4.0	144.7	30.0	295	0.445	1477	10.0	90.0	3.61	15.68	22	−0.0083	−36
H-2	Modified	H_2/CH_4	3.1	173.2	47.0	294	0.434	1448	11.7	88.3	3.88	20.25	26	−0.0119	−22
H-3	Modified	H_2/CH_4	3.8	172.4	38.6	295	0.526	1643	9.3	90.7	4.34	19.01			
H-4	Modified	H_2/CH_4	5.1	168.4	27.8	293	0.438	1463	9.5	90.5	2.99	13.59	16	−0.0124	−27
H-5	Modified	H_2/CH_4	3.0	111.6	30.6	293	0.381	1342	7.8	92.2	3.42	15.93	22	−0.0079	−33
H-6	Modified	H_2/CH_4	5.1	170.5	38.7	412	0.420	1517	10.7	89.3	5.23	21.28	18	−0.0081	−38
H-7	Modified	H_2/CH_4	5.2	169.1	39.0	410	0.547	1766	11.9	88.1	5.30	22.22	14	−0.0083	−37
H-8	Modified	H_2/CH_4	7.1	171.1	27.7	414	0.346	1356	9.9	90.1	3.20	14.71	14	−0.0078	−47
H-9	Modified	H_2/CH_4	7.1	168.2	28.0	411	0.485	1650	10.9	89.1	3.49	16.64	7	−0.0065	−56
H-10	Modified	H_2	7.1	167.7	27.7	414	0.330	1348	0.0	100.0	2.87	15.43	9	−0.0087	−41
Nonreacting															
NR-5	Modified	—	4.0	171.9	46.2	435	—	—	—	—	—	—	—	−0.0037	−96
NR-6	Modified	—	5.0	170.1	36.2	432	—	—	—	—	—	—	—	−0.0042	−81

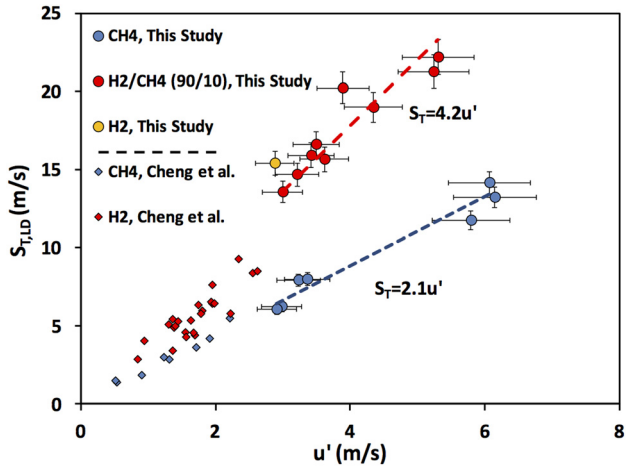

Fig. 14 $S_{T,LD}$ as a function of u'

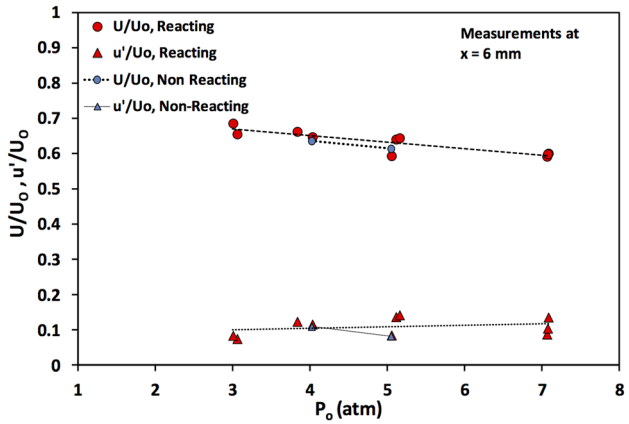

Fig. 15 *U/Uo* and u'/U_O near the nozzle exit for nonreacting and reacting flows for LSI-P2

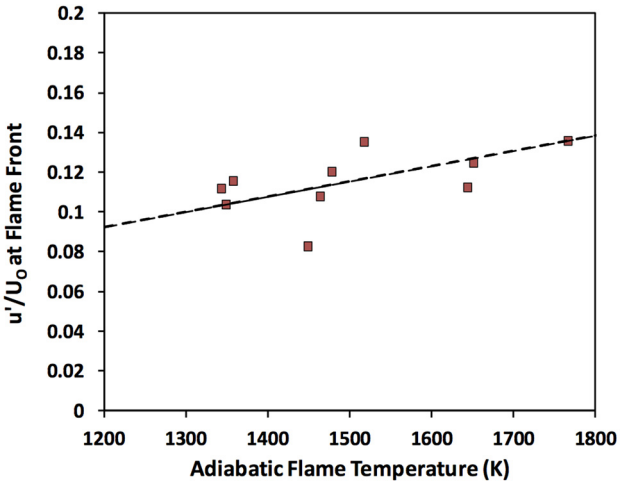

Fig. 16 Turbulence intensity at leading edge of flame as a function of *AFT* for flames H-1 through H-10

implies that the only two parameters that control $S_{T,LD}$ are the fuel composition and the turbulence level. If any dependency on pressure or temperature does exist, they are within the experimental uncertainty of the data. A single test was also conducted with pure hydrogen in this study. This point (in orange) has a $S_{T,LD}$ measured for this test was about 14% higher than the $S_{T,LD}$ for the 90/10 blend at similar inlet conditions.

The higher turbulent flame speed for high-hydrogen blends over methane base fuels are expected given hydrogen's higher propensity to flashback. However, the lack of pressure and inlet temperature dependence at first may be rather unexpected because of the strong influence that P_o and T_o have on the flashback limits. This counterintuitive result can be explained by the effect the inlet conditions have on the flow field upstream of the flame. Figure 15 plots the normalized mean velocity near nozzle exit ($x = 6$ mm) versus P_o for reacting high-hydrogen and nonreacting LDV tests (from Fig. 6). U/U_o is seen to decrease with pressure for both reacting and nonreacting flows. In the case of reacting flows, this decrease in mean velocity allows the flame to anchor closer to the nozzle rim. This is consistent with the observations that flames anchor closer to the nozzle with increasing pressure mentioned earlier. Comparison of the values of U/U_o and the rate of decrease with P_o between the reacting and nonreacting flows show the two cases to be the same. This indicates that the velocity dependence on pressure is not a result of flame/flow interactions. The turbulence intensity u'/U_o does not show any change with P_o, which would indicate that $S_{T,LD}$ would remain constant for a given bulk velocity. This also consistent with the turbulent flame speed measurements.

Observations with changes in inlet temperature show that increasing T_o pushes the flame away from the nozzle. Unfortunately, the LDV testing was not performed over a wide enough inlet temperatures range (because of seeder limitations to relatively low temperatures) to see if U/U_o is also dependent on inlet temperature. It is conjectured that an opposite effect would have been observed for increasing in T_o. That is, U/U_o would increase with T_o, but this remains to be proven. If this was the case, it would explain the dependence of the flashback limit on inlet temperature.

While u'/U_o did not show any dependence on P_o or T_o in the high-hydrogen tests, u'/U_o at x_f was found to increase with *AFT* as shown in Fig. 16. The turbulence intensity dependence on flame temperature can be from two possible sources. First, increasing heat release with *AFT* may create fluctuations in the flow that generate additional turbulence. Second, Johnson et al. [15] have shown that divergence rate upstream of the flame increases with flame temperature due to the thermal expansion of the reactants upon crossing the flame front. This increase in divergence/strain can supply the flow field with additional turbulent kinetic energy, which in turn increases u'/U_o. Given that $S_{T,LD}$ is so strongly dependent upon u', this flame generated turbulence will, subsequently, increase $S_{T,LD}$. Therefore, it is believed that the observed upstream propagation of the flame with u' observed is a result of the $S_{T,LD}$ indirectly increasing with *AFT* through u'.

Conclusions

Flow field and flashback measurements were performed in a flame stabilized with a low-swirl injector and a sudden expansion nozzle in quartz-lined combustor in an optically accessible test rig using methane and high-hydrogen fuels. The key findings of this study are:

- Flashback occurs when the leading edge of the lifted flame ingresses within the combustor nozzle.
- Increasing P_o and *AFT* increase the propensity for flashback, whereas increasing T_o and U_o decrease it.
- The propensity of flashback is dependent upon the proximity of the flame to the nozzle that is itself dependent upon the parameters P_o, T_o, *AFT*, and U_o.
- The turbulent flame speed is only a function of the turbulence intensity and fuel composition.
- The flow field itself (in both reacting and nonreacting flows) can be affected by changes in U_o, P_o, and T_o.

The results of this study are useful in showing the connection between flow field and flame speed with flame position and, subsequently, flashback limits. To the authors' knowledge this study is the first detailed analysis of a reacting flow field stabilized by an LSI at relevant gas turbine conditions with high-hydrogen fuels. Hopefully this information will be useful for design use for future generation gas turbine combustors or also for simulation validation. The authors welcome any future collaboration with industry or academia regarding low-swirl combustion.

Acknowledgment

The authors would like to thank the students and staff at the UCICL for their assistance, specifically Adrian Narvaez, Joe Velasco, Kyle Dykman, Adam Silver, Guillermo Gomez, Rich Hack, and Professor Scott Samuelsen. The authors also thank Dr. David Littlejohn (LBNL) and Dr. Bobby Noble (Georgia Tech) for helpful discussions with the experimental setup. Most of the experimental setup and analysis was supported by Contract No. 500-08-034 with the California Energy Commission (CEC) under the direction of Marla Mueller. The LDV system was purchased with funding from the Naval Office of Research. LBNL authors were supported by the Assistant Secretary for Fossil Energy, Advanced Turbines Program, of the U.S. Department of Energy under Contract No. DE-AC02-05CH11231

Nomenclature

a_x = normalized axial divergence rate
AFT = adiabatic flame temperature (K)
K = fuel dependent constant
P_o = inlet pressure (atm)
r = radial distance from axis
R = combustor radius
$S_{T,LD}$ = local displacement turbulent flame speed (m/s)
T_o = inlet mixture temperature (K)
U, V = mean axial and radial velocity, respectively (m/s)
U_o = bulk velocity through premixer (m/s)
u', v' = rms axial and radial velocity, respectively (m/s)
x = axial distance from nozzle exit
x_f = lift-off height
x_O = virtual origin
Δp = pressure drop
φ = equivalence ratio

References

[1] Lieuwen, T. V., Yang, V., and Yetter, R., eds., 2009, *Synthesis Gas Combustion*, CRC Press, Boca Raton, FL.
[2] Lieuwen, T., McDonell, V., Petersen, E., and Santavicca, D., 2008, "Fuel Flexibility Influences on Combustor Blowout, Flashback, Autoignition, and Stability," ASME J. Eng. Gas Turb. Power., **130**(1), p. 011506.
[3] Bell, J., Cheng, R., Day, M., and Shepherd, I., 2007, "Numerical Simulation of Lewis Number Effects on Lean Premixed Turbulent Flames," Proc. Combust. Inst., **31**, pp. 1309–1317.
[4] Baum, M., Poinsot, T., Haworth, D., and Darabiha, N., 1994, "Direct Numerical Simulations of $H_2/O_2/N_2$ Flames With Complex Chemistry in Two-Dimensional Turbulent Flows," J. Fluid Mech., **281**, pp. 1–32.
[5] Driscoll, J., 2008, "Turbulent Premixed Combustion: Flamelet Structure and Its Effect on Turbulent Burning Velocities," Prog. Eng. Combust. Sci., **34**(1), pp. 91–134.
[6] Cheng, R., 2009, "Turbulent Combustion Properties of Premixed Syngas," *Synthesis Gas Combustion*, T. Lieuwen, V. Yang, and R. Yetter, eds., CRC Press, Boca Raton, FL, Ch. 5.
[7] Daniele, S., Jansohn, P., and Boulouchos, K., 2009, "Flame Front Characteristics and Turbulent Flame Speed of Lean Premixed Syngas Combustion at Gas Turbine Relevant Conditions," ASME Paper No. GT2009-59477.
[8] Marshall, A., Venkateswaran, P., Noble, D., Seitzman, J., and Lieuwen, T., 2012, "Pressure Effects on the Turbulent Consumption Speeds of High H_2 Mixtures," ASME Paper No. GT2012-68305.
[9] Cheng, R., Littlejohn, D., Nazeer, W., Smith, K., 2008, "Laboratory Studies of the Flow Field Characteristics of Low-Swirl Injectors for Adaptation to Fuel-Flexible Turbine," ASME J. Eng. Gas Turb. Power, **130**(2), p. 021501.
[10] Koyama, M., and Tachibana, S., "Technical Applicability of Low-Swirl Fuel Nozzle for Liquid-Fueled Industrial Gas Turbine Combustor," Fuel, **107**, pp. 766–776.
[11] Chan, C., Lau, K., Chin, W., and Cheng, R., 1992, "Freely Propagating Open Premixed Turbulent Flames Stabilized by Swirl," Symp. (Int.) Combust., **24**(1), pp. 511–518.
[12] Littlejohn, D., and Cheng, R., 2007, "Fuel Effects on a Low-Swirl Injector for Lean Premixed Gas Turbines," Proc. Combust. Inst., **31**(2), pp. 3155–3162.
[13] Cheng, R., Yegian, D., Miyasato, M., Samuelsen, G., Benson, C., Pellizzari, R., and Loftus, P., 2000, "Scaling and Development of Low-Swirl Burners for Low-Emission Furnaces and Boilers," Proc. Combust. Inst., **28**, pp. 1305–1313.
[14] Smith, K., Therkelsen, P., Littlejohn, D., Ali, S., and Cheng, R., 2010, "Conceptual Studies of Fuel-Flexible Low Swirl Combustion Systems for the Gas Turbine in Clean Coal Powerplants," ASME Paper No. GT2010-23506.
[15] Johnson, M., Littlejohn, D., Nazeer, W., Smith, K., and Cheng, R., 2005, "A Comparison of the Flow Fields and Emissions of High-Swirl Injectors and Low-Swirl Injectors for Lean Premixed Gas Turbines," Proc. Combust. Inst., **30**, pp. 2867–2874.
[16] Nazeer, W. Smith, K., Sheppard, P., Cheng, R., and Littlejohn, D., 2006, "Full Scale Testing of a Low Swirl Fuel Injector Concept for Ultra-Low NO_x Gas Turbine Combustion Systems," ASME Paper No. GT2006-90150.
[17] Cheng, R., Littlejohn, D., Strakey, P., and Sidwell, T., 2007, "Laboratory Investigations of a Low-Swirl Injector With H_2 and CH_4 at Gas Turbine Conditions," Proc. Combust. Inst., **31**, pp. 3155–3162.
[18] Littlejohn, D., Cheng, R., Noble, D., and Lieuwen, T., 2010, "Laboratory Investigations of Low-Swirl Injectors Operating With Syngases," ASME J. Eng. Gas Turb. Power, **132**(1), p. 011502.
[19] Cheng, R., and Littlejohn, D., 2008, "Laboratory Study of Premixed H_2-Air and H_2-N_2-Air Flames in a Low-Swirl Injector for Ultralow Emissions Gas Turbine," ASME J. Eng. Gas Turb. Power, **130**(3), p. 031503.
[20] Fritz, J., Kröner, M., and Sattelmayer, T., 2004, "Flashback in a Swirl Burner With Cylindrical Premixing Zone," ASME J. Eng Gas Turb. Power, **126**(2), pp. 276–283.
[21] Eichler, C., Baumgarther, G., and Sattelmayer, T., 2012, "Experimental Investigation of Turbulent Boundary Layer Flashback Limits for Premixed Hydrogen-Air Flames Confined in Ducts," ASME J. Eng. Gas Turb. Power, **134**(1), p. 011502.
[22] Therkelsen, P., Werts, T., McDonell, V., and Samuelsen, S., 2009, "Analysis of NO_X Formation in a Hydrogen Fueled Gas Turbine," ASME J. Eng. Gas Turb. Power, **131**(3), p. 031507.
[23] Beerer, D., McDonell, V., Therkelsen, P., and Cheng, R., 2012, "Flashback, Turbulent Displacement Flame Speeds, Blow-Out and Emissions Measurements in a Hydrogen and Methane Fired Low-Swirl Injector at Elevated Pressures and Temperatures," ASME Paper No. GT2012-68216.
[24] Beerer, D., 2013, "Combustion Characteristics and Performance of Low-Swirl Injectors With Natural Gas and Alternative Fuels at Elevated Pressures and Temperatures," Ph.D. dissertation, Mechanical and Aerospace Dept., University of California, Irvine, CA.
[25] Therkelsen, P., Littlejohn, D., and Cheng, R., 2012, "Parametric Study of Low-Swirl Injector Geometry on its Operability," ASME Paper No. GT2012-68436.
[26] Therkelsen, P., Littlejohn, D., Cheng, R., Portillo, J., and Martin, S., 2010, "Effect of Combustor Inlet Geometry on Acoustic Signature and Flow Field Behavior of the Low-Swirl Injector," ASME Paper No. GT2010-23498.
[27] Davis, D., Therkelsen, P., Littlejohn, D., and Cheng, R., 2013, "Effects of Hydrogen on the Thermo-Acoustics Coupling Mechanisms of Low-Swirl Flames in a Model Gas Turbine Combustor," Proc. Combust. Inst., **34**(2), pp. 3135–3143.
[28] Noble, D., Zhang, Q., Shareef, A., Tootle, J., Meyers, A., and Lieuwen, T., 2006, "Syngas Mixture Composition Effects Upon Flashback and Blow Out," ASME Paper No. GT2006-90470.
[29] Kröner, M., Fritz, J., and Sattelmayer, T., 2003, "Flashback Limits for Combustion Induced Vortex Breakdown in a Swirl Burner," ASME J. Eng. Gas Turb. Power, **125**, pp. 693–700.
[30] Eggenspieler, G., Strakey, P., and Sidwell, T., 2008, "Experimental and Numerical Study of Flashback in the SimVal Combustion Chamber," 46th AIAA Aerospace Sciences Meeting and Exhibit, Reno, NV, AIAA Paper No. 2008-1025.
[31] Daniele, S., Jansohn, P., and Boulouchos, K., 2010, "Flashback Propensity of Syngas Flames at High Pressure: Diagnostics and Control," ASME Paper No. GT2010-23456.
[32] Cheng, R., 1984, "Conditional Sampling of Turbulence Intensities and Reynolds Stresses in Premixed Turbulent Flames," Combust. Sci. Tech., **41**, pp. 109–142.